

Discovery of an anomalous non-evaporating sub-nanometre water layer in open environment

Zhijie Li,^{1,2,*} Xi Kong,^{3,*} Haoyu Sun,^{1,2} Guanyu Qu,^{1,2} Pei Yu,^{1,2} Tianyu Xie,^{1,2} Zhiyuan Zhao,^{1,2} Guoshen Shi,⁴ Ya Wang,^{1,2,5} Fazhan Shi,^{1,2,5,6,†} and Jiangfeng Du^{1,2,5,7,‡}

¹CAS Key Laboratory of Microscale Magnetic Resonance and School of Physical Sciences, University of Science and Technology of China, Hefei 230026, China

²Anhui Province Key Laboratory of Scientific Instrument Development and Application, University of Science and Technology of China, Hefei 230026, China

³The State Key Laboratory of Solid State Microstructures and Department of Physics, Nanjing University, 210093 Nanjing, China

⁴Shanghai Applied Radiation Institute, State Key Laboratory Advanced Special Steel, Shanghai University, Shanghai 200444, China

⁵Hefei National Laboratory, University of Science and Technology of China, Hefei 230088, China

⁶School of Biomedical Engineering and Suzhou Institute for Advanced Research, University of Science and Technology of China, Suzhou 215123, China

⁷Institute of Quantum Sensing and School of Physics, Zhejiang University, Hangzhou 310027, China

Water exhibits complex behaviors as a result of hydrogen bonding, and low-dimensional confined water plays a key role in material science, geology, and biology science. Conventional techniques like STM, TEM, and AFM enable atomic-scale observations but face limitations under ambient conditions and surface topographies. NV center magnetic resonance technology provides an opportunity to overcome these limitations, offering non-contact atomic-scale measurements with chemical resolution capability. In this study, a nanoscale layer dissection method was developed utilizing NV center technology to analyze water layers with diverse physicochemical properties. It unveiled the presence of a non-evaporating sub-nanometer water layer on a diamond surface under ambient conditions. This layer demonstrated impervious to atmospheric water vapor and exhibited unique electronic transport mediated via hydrogen bonding. These findings provide new perspectives and a platform for studying the structure and behavior of low-dimensional water, as well as the surface properties influenced by adsorbed water under native conditions.

Water, as the most valuable natural resource, intricately influences life sciences, sculpting the Earth's landscape and captivating the scientific community's interest. Despite its simple chemical structure, the presence of hydrogen (H) bonds leads to numerous phases; currently, there are 17 experimentally confirmed ice polymorphs and several more predicted computationally [1]. And among them, low-dimensional adsorbed water or confined water often plays a pivotal role, such as the importance of confined water in the structural and dynamic functions of molecular cell biology [2, 3]. However, due to the influences of restricted dimensions, polarities of restricted surfaces, static electricity, hydrophobic forces, H bonding, etc. [4, 5], low-dimensional water exhibits surprisingly rich and diverse phase behaviors [5, 6]. Hence, investigating and characterizing the structure and properties of low-dimensional interface water have emerged as crucial research areas.

Low-dimensional water has been extensively researched under various conditions utilizing techniques such as scanning tunneling microscopy (STM) [7–9], transmission electron microscopy (TEM) [10, 11], and atomic force microscopy (AFM) [12–14]. These methods

facilitate the direct observation of the structural characteristics of low-dimensional water at an atomic scale. However, challenges arise due to interactions involving voltage, charge, and van der Waals forces, making it difficult to entirely avoid impacting the low-dimensional water layers. Another critical issue is the complexity of achieving spatial resolution while analyzing the chemical environment in terms of atomic species and scale [15, 16], hindering the direct correlation of other properties and structural features of low-dimensional water. Fortunately, the emerging magnetic resonance technique based on nitrogen-vacancy (NV) center in diamond presents a unique opportunity. NV center enable non-contact atomic-scale measurements utilizing magnetic resonance technique, providing atomic spatial resolution without interfering with the sample itself [17, 18]. Most importantly, NV centers offer chemical shift resolution [19, 20] in nuclear magnetic resonance spectroscopy, delivering crucial information for property detection.

In this study, we developed a nanoscale liquid dissection method (Fig. 1(a)) to analyze and differentiate surface water using NV center magnetic resonance technology. Water layers with diverse physical and chemical properties can be separated or eliminated through physical and chemical means. The capabilities of NV sensors in nanoscale magnetic resonance [15] enable precise analysis of nuclear magnetic resonance (NMR) spectra and investigation of their structures, including the ex-

*These authors contributed equally to this work.

†Electronic address: fzshi@ustc.edu.cn

‡Electronic address: djf@ustc.edu.cn

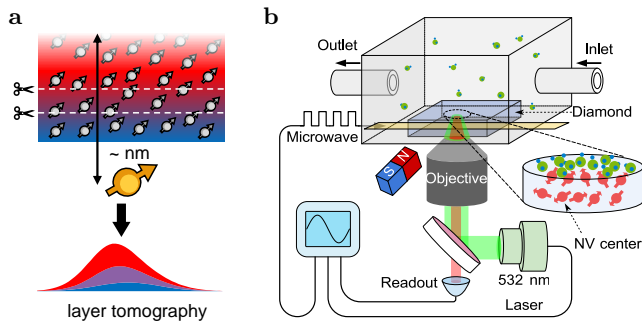


FIG. 1: (a) Dissection of the adsorbed water layer on the diamond surface. By manipulating the ambient environment, nanoscale adsorbed layers with different physicochemical properties can be sequentially removed. Using a sensor located a few nanometers beneath the surface, the characteristics of each layer can be precisely measured. (b) Adsorption analysis setup based on NV center. The sample chamber is designed flow-through for vapor or liquid coming into contact with the diamond surface.

amination of interactions among different water layers (Fig. 1(a)). Under an open ambient condition, an ice-like sub-nanometer water layer was observed on the diamond surface. Remarkably, we observed that this water layer remained isolated from atmospheric water vapor and upper adsorbed water layer throughout the experiment duration. Subsequently, we conducted a comprehensive examination and deliberation on this unexpected finding, leading to the formulation of a plausible explanatory model.

We utilized a 50 μm thick ultrapure diamond film with a nitrogen concentration of 5 ppb as the substrate and fabricated near-surface NV centers as sensors via ion implantation technology [15], with a depth of approximately 5-10 nm. The sensor was positioned inside a quartz enclosure, and the environmental conditions of the diamond surface are regulated by introducing gas or liquid into it, as illustrated in Fig. 1(b). Using optically detected magnetic resonance (ODMR) technique, the electron spin of NV centers is controlled via a coplanar microwave waveguide closely attached to the underside of the diamond. Concurrently, lasers are aimed at the shallow NV centers through the central aperture of the waveguide for the purpose of initializing and reading the NV centers. The interfacial nuclear spins are weakly coupled to the shallow NV centers, therefore, NMR spectra can be acquired via controls and readouts of the NV center. For proton detection, we used dynamical decoupling sequences as shown in the inset of Fig. 2(a). The pulse sequence used was the standard XY4-N sequence, where NV spin flips were modulated by π pulses at intervals of τ to detect the radio frequency signal at $\pi\tau$ frequency, corresponding to $\omega_L = \gamma_H B_0$, with γ_H representing the gyromagnetic ratio of protons and B_0 denoting the static magnetic field applied. Based on the NMR spectra, information such as proton frequency, relaxation time, and quantity at the interface can be elucidated, as depicted in

Fig. 2(a). Experimental studies were carried out under varying environmental conditions, covering H_2O vapor, D_2O vapor, and corresponding liquid environments. The near-saturated vapor was generated by passing ultrapure nitrogen (> 99.9999%) through H_2O or D_2O water tank. By manipulating these conditions, the isotopes of the adsorbed layers were modified for distinct proton spectrum measurements. The proton spectrum showed the most prominent signal in the H_2O vapor environment, as illustrated in Fig. 2(a). Subsequent alteration of the D_2O vapor led to an exchange of water within the adsorption layer, resulting in a noticeable decrease in proton signal. Furthermore, the introduction of liquid D_2O further decreased the proton content, indicating the existence of intricate water layers with varying characteristics on the surface. Different substitutions occurred under different operational conditions, enabling a systematic exploration of the detailed spectral structures of complex water layers with diverse properties.

Firstly, we monitored the temporal evolution of proton spectral intensity as water vapor isotopes underwent exchange in the evolving environment (proton substituted for deuterium and vice versa), as depicted in Fig. 2(b). The diamond was initially immersed in a H_2O setting, dried, and subsequently exposed to a H_2O vapor atmosphere. A sufficient duration of measurement was taken to attain a stable state. After about 250 minutes, the environment was switched to D_2O vapor, resulting in a gradual decline in proton spectral intensity. Following a measurement duration of around 500 minutes, reintroduction of H_2O vapor led to gradual signal recovery in the proton nuclear magnetic spectrum (Fig. 2(b)). The transition from one stable state to another required approximately 3 hours. This suggests that a layer of adsorbed water undergoes gradual exchange with water molecules in the gas phase.

Subsequently, the diamond was immersed in D_2O liquid, resulting in a further reduction in proton spectral intensity, yet not reaching zero (Phase II in Fig. 2(c)). The residual proton signals are likely attributed to various sources, including hydroxyl groups (-OH) present on the surface of oxidized diamond, as well as hydrogen-containing functional groups bound within subsurface defect regions (e.g., $-\text{CH}_2$ and $-\text{CH}_3$). The introduction of H_2O vapor caused an increase in the proton spectral intensity (Phase III in Fig. 2(c)), although it remained significantly lower than the initial proton spectrum in the protonated surface state (Phase V in Fig. 2(c)).

These two experiments elucidate that certain adsorbed water molecules evade exchange with the gaseous environment even over a long experimental duration (record for a week). Consequently, two distinct layers of water adsorption are proposed (Fig. 2(d)): a loosely bound layer capable of atmospheric exchange and another layer activated solely upon substantial liquid water introduction. Through spectral amplitude analysis, it was determined that the thickness of this water layer is extremely thin, measuring less than 1 nm [21], thereby

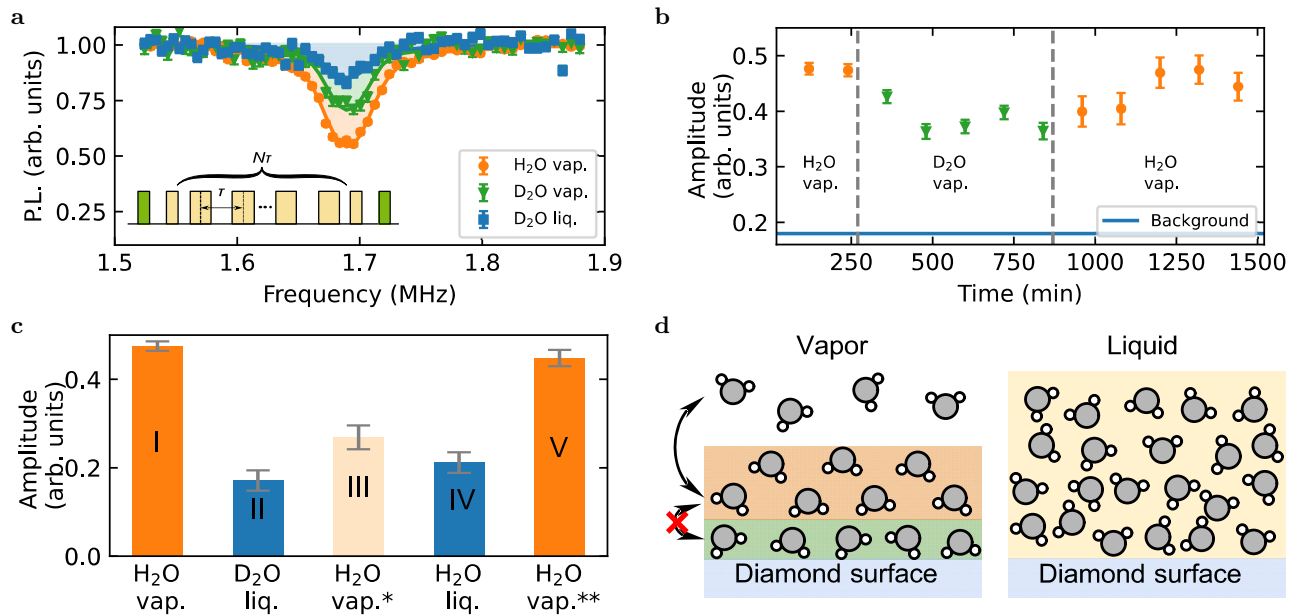


FIG. 2: (a) Changing the environment allows for the replacement of isotopes in the water adsorption layer on the diamond surface. By altering the isotopes of the input gas, the isotopes of the water in the adsorption layer can be modified. Experimental proton NMR spectra reveal differences in signal amplitudes for H₂O vapor (orange), D₂O vapor (green), and D₂O liquid (blue), demonstrating the influence of physical state and surface interactions on spectral dependence. An inset illustrates the NV-based NMR control sequence (XY4-N), where the time interval τ in the control sequence determines the detection frequency at $1/2\tau$. (b) The resonant peak amplitudes in proton NMR spectra exhibit temporal variations under different vapor environments. The orange and green data points in the figure correspond to measurements taken under H₂O and D₂O vapor conditions, respectively. The background signal (blue line), which was the surface state initialized by D₂O liquid, is used as the control in the study. The transition in vapor environments is indicated by the dashed line. (c) Comparison of the steady-state amplitudes of resonance peaks under changing environmental conditions involves resetting the surface to a proton surface (I) using H₂O liquid, replacing it with a deuterium surface (II) through the addition of D₂O liquid, and subsequently introducing H₂O vapor (III), H₂O liquid (IV), and H₂O vapor (V) in a sequence. (d) The schematic diagram depicting molecules on the diamond surface illustrates the distribution of the water layer on the diamond under vapor and liquid states. The left side represents vapor conditions, while the right side represents liquid conditions. It was observed that the low-dimensional water layer identified does not exchange with external water molecules under vapor conditions but can be activated under liquid conditions.

qualifying it as a low-dimensional water (LDW) layer. Moreover, an additional non-exchangeable proton layer, attributable to surface-residual hydrogenous functional groups, persists even upon liquid water introduction. This non-exchangeable hydrogen component, irrelevant to our study, will be factored out as background in subsequent analyses, with focus directed towards delineating the characteristics of the two distinct adsorbed water layers.

In order to investigate the impacts of the abnormal no-exchange layer further, we employed high-resolution NMR techniques to analyze the intricate structure of proton spin on the diamond surface in both H₂O and D₂O vapor environments. Employing correlation spectroscopy methods [22, 23] (Fig. 3(a)), we enhanced the spectral resolution from \sim MHz to the \sim kHz range. Fig. 3(b) exhibit the frequency domain NMR spectra in the H₂O and D₂O vapor environments. In both cases, a distinct narrow spectral line is observed, which can be ascribed to surface proton-containing functional groups. Their spin-free neighboring environment or the rotational mobilities

results in the reduction of interactions [22, 24, 25], leading to a narrow spectral width. In the D₂O vapor context of this comparative study, the upper loose layer was replaced with deuterium, causing its absence in the proton spectrum and a consequent reduction in the central peak intensity. Notably, we observed novel peaks deviating from the central peak, displaying a negative shift exceeding the spectrum linewidth in both D₂O and H₂O vapor environments, suggesting a potential chemical shift-like shielding effect. The observed frequency shift is 3 kHz in the D₂O vapor environment and 16 kHz in the H₂O vapor environment, displaying a roughly 1% deviation at a magnetic field strength of 39.7 mT. This deviation indicates that there is stronger interaction between the LDW layer and the adsorbed water layer in the H₂O vapor environment, leading to a stronger shielding effect.

The redshift observed in nuclear spins could be attributed to electron shielding effects. To validate this, an investigation into the characteristics of surface electrons is essential. Fortunately, the NV center, functioning as a versatile quantum sensor, can employ double

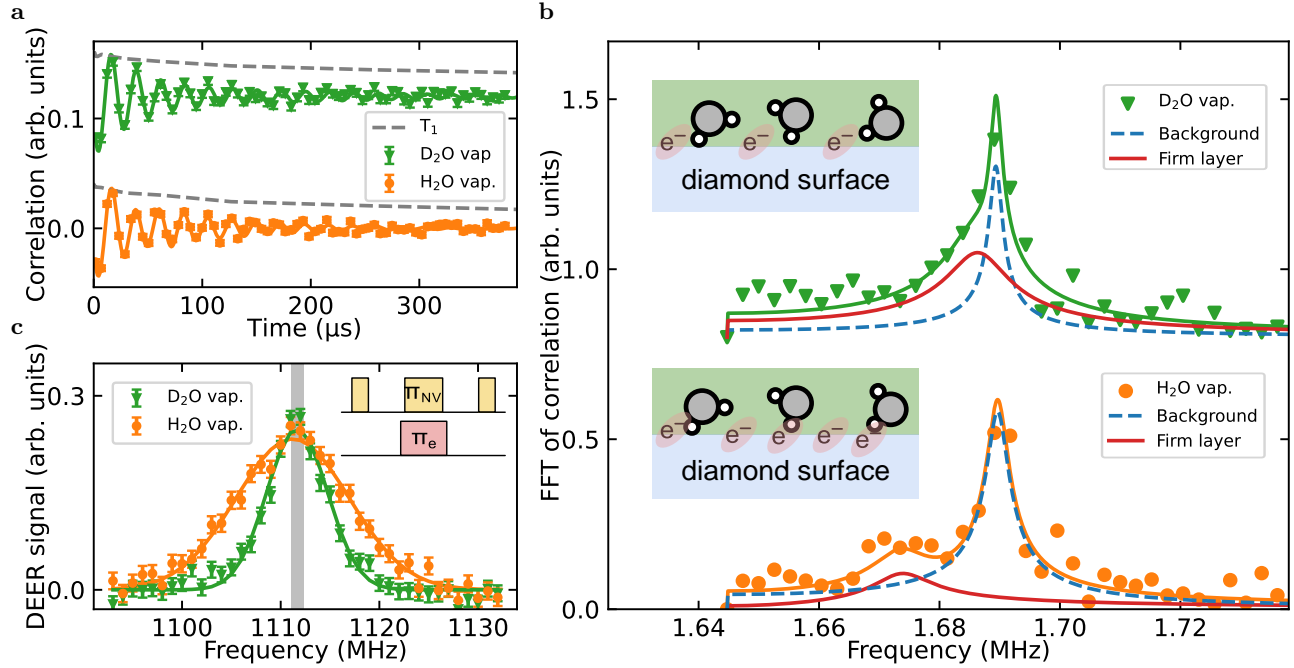


FIG. 3: (a) Correlation signal obtained in D₂O vapor or H₂O vapor conditions. The sampling interval was set to 9.25 times the proton precession period. Corresponding NV center relaxations are shown by gray dashed lines. (b) The FFT amplitudes of the correlation signals shown in (a). The spectra reveal two primary frequency components of proton nuclei: a sharp peak corresponding to the slowly decaying signal at the proton precession frequency, and a broadened peak associated with the fast decaying signal in the firmly adsorbed layer, which shows a redshift relative to the proton precession frequency. The insets illustrate the mechanism of the redshift caused by paramagnetic shielding, with deuterium atoms highlighted in red. (c) DEER spectrum under D₂O vapor or H₂O vapor conditions. The diamond surface was H₂O liquid treated before experiment. The inset displays the pulse used in DEER experiments (laser pulses are not shown). The full width at half maximum of the DEER spectra is fitted to 7.2(3) MHz and 13.4(5) MHz, respectively, with a Gaussian lineshape. The upper bound of power broadening is indicated by a gray bar.

electron–electron resonance (DEER) techniques to perform nanoscale electron spin resonance (ESR) measurements with shallow NV centers [24]. Fig. 3(c) demonstrates the ESR spectra obtained under H₂O and D₂O vapor conditions following the diamond surface pretreatment with H₂O liquid. The ESR spectrum exhibits a noticeable broadening in the presence of H₂O vapor. These observations imply a greater electron density near the NV detector, offering additional evidence that the electron contributes to the redshift in nuclear spin resonance frequency from an alternative viewpoint.

The phenomenon is attributed to the localization of protons, which is known as nuclear quantum effects (NQE). NQE's presence results in an approximate 9% increase in the number of hydrogen bonds in deuterated water compared to regular water [26], thereby boosting electron adsorption capacity and causing significant spectral changes in LDW under both H₂O and D₂O vapor environments. This process diminishes the electron affinity of the diamond interface, as evidenced by the concurrent decrease in contrast of NV centers (see Fig. 4 (a, b)). Transitioning to a D₂O vapor environment gradually diminishes the NV center contrast, which can recover upon reverting to a H₂O vapor setting. This reproducible effect underscores the heightened possibility of

electron loss within illuminated NV centers under H₂O vapor conditions. It partially elucidates the potential electron sources, with potential contributions from other dark defects [27], and the electron conductivity beyond the diamond [28], as depicted in Fig. 4(c). In H₂O settings, due to the NQE effect, more electrons may accumulate in the LDW layer, enhancing the shielding effect on protons. This interpretation correlates with the observed variations in NMR spectral chemical shifts and the broadening of ESR spectra.

In conclusion, our method, based on the NV center, facilitates surface analysis to investigate the properties of interfacial water. By systematically substituting isotopes in various water layers, we distinguished different water layers and conducted separate analyses of the magnetic resonance spectrum, including nanoscale NMR and ESR. Our research revealed the existence of an anomalous water layer, just one molecular layer thick, on the diamond surface at room temperature. This layer exhibits ice-like properties and remains stable without exchanging with external water vapor. High-resolution nanoscale NMR analysis revealed significant chemical shifts of protons within this unique water layer, likely arising from the nuclear quantum effect of D₂O H bond. These findings provide valuable insights and experimental pathways for

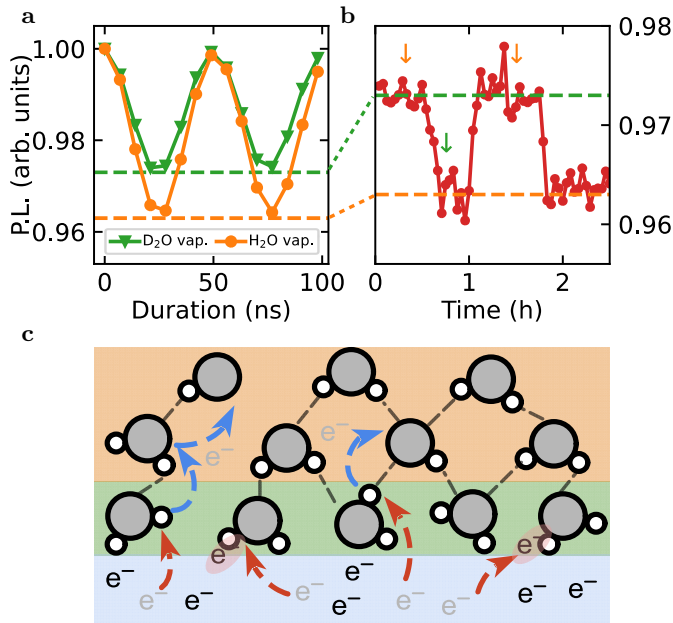


FIG. 4: (a) Rabi oscillation of NV center in H₂O or D₂O vapor conditions. (b) The variation of photoluminescence difference between NV center spin states during condition transitions. The orange (H₂O vapor) and green (D₂O vapor) arrows indicate when the corresponding transition begins. (c) Electron transfer model at diamond surface. The surface electrons are prone to transfer into the H bond network in the adsorption layer. The H bond energy affects the electron conductance in the network, resulting in different surface residual electron densities.

examining low-dimensional water structures and properties across the fields of materials science, geology, and biology.

Acknowledgements: We thank Prof. Sujing Wang and Prof. Jihu Su for helpful discussions. This work was supported by the National Natural Science Foundation of China (Grant No. T2125011), the CAS (Grants No. GJJSTD20200001, No. YSBR-068), Innovation Program for Quantum Science and Technology (Grants No. 2021ZD0302200, No. 2021ZD0303204), New Cornerstone Science Foundation through the XPLOER PRIZE, and the Fundamental Research Funds for the Central Universities.

Author contributions: J.D. and F.S. supervised the project and proposed the idea; F.S., Z.L. and X.K. designed the experiments; Z.L. performed the experiments; H.S., P.Y. and Y.W. prepared the diamond sample; Z.L., X.K. and F.S. wrote the manuscript. All authors discussed and analyzed the data.

-
- [1] C. G. Salzmann, *The Journal of Chemical Physics* **150**, 060901 (2019).
- [2] P. Ball, *Chem. Rev.* **108**, 74 (2008).
- [3] Charles. Tanford, *J. Am. Chem. Soc.* **84**, 4240 (1962).
- [4] K. Wu, Z. Chen, J. Li, X. Li, J. Xu, and X. Dong, *Proc. Natl. Acad. Sci.* **114**, 3358 (2017).
- [5] M. B. Davies, A. Rosu-Finsen, C. G. Salzmann, and A. Michaelides, *How Crystalline is Low-Density Amorphous Ice?* (2024), 2305.03057.
- [6] V. Kapil, C. Schran, A. Zen, J. Chen, C. J. Pickard, and A. Michaelides, *Nature* **609**, 512 (2022).
- [7] S. Nie, P. J. Feibelman, N. C. Bartelt, and K. Thürmer, *Phys. Rev. Lett.* **105**, 026102 (2010).
- [8] S. Maier, B. A. J. Lechner, G. A. Somorjai, and M. Salmeron, *J. Am. Chem. Soc.* **138**, 3145 (2016).
- [9] C. Lin, N. Avidor, G. Corem, O. Godsi, G. Alexandrowicz, G. R. Darling, and A. Hodgson, *Phys. Rev. Lett.* **120**, 076101 (2018).
- [10] Ç. Ö. Girit, J. C. Meyer, R. Erni, M. D. Rossell, C. Kisielowski, L. Yang, C.-H. Park, M. F. Crommie, M. L. Cohen, S. G. Louie, et al., *Science* **323**, 1705 (2009).
- [11] G. Algara-Siller, O. Lehtinen, F. C. Wang, R. R. Nair, U. Kaiser, H. A. Wu, A. K. Geim, and I. V. Grigorieva, *Nature* **519**, 443 (2015).
- [12] J. Peng, D. Cao, Z. He, J. Guo, P. Hapala, R. Ma, B. Cheng, J. Chen, W. J. Xie, X.-Z. Li, et al., *Nature* **557**, 701 (2018).
- [13] A. Shiotari and Y. Sugimoto, *Nat Commun* **8**, 14313 (2017).
- [14] R. Ma, D. Cao, C. Zhu, Y. Tian, J. Peng, J. Guo, J. Chen, X.-Z. Li, J. S. Francisco, X. C. Zeng, et al., *Nature* **577**, 60 (2020).
- [15] J. Du, F. Shi, X. Kong, F. Jelezko, and J. Wrachtrup, *Rev. Mod. Phys.* **96**, 025001 (2024).
- [16] S. A. Claridge, J. J. Schwartz, and P. S. Weiss, *ACS Nano* **5**, 693 (2011).
- [17] P. Wang, S. Chen, M. Guo, S. Peng, M. Wang, M. Chen, W. Ma, R. Zhang, J. Su, X. Rong, et al., *Sci. Adv.* **5**, eaau8038 (2019).
- [18] M. S. Grinolds, M. Warner, K. D. Greve, Y. Dovzhenko, L. Thiel, R. L. Walsworth, S. Hong, P. Maletinsky, and A. Yacoby, *Nat Nano* **9**, 279 (2014).
- [19] M. H. Abobeih, J. Randall, C. E. Bradley, H. P. Bartling, M. A. Bakker, M. J. Degen, M. Markham, D. J. Twitchen, and T. H. Taminiau, *Nature* **576**, 411 (2019).
- [20] N. Aslam, M. Pfender, P. Neumann, R. Reuter, A. Zappe, F. F. de Oliveira, A. Denisenko, H. Sumiya, S. Onoda, J. Isoya, et al., *Science* **357**, 67 (2017).
- [21] [Supplementary Material](#).
- [22] T. Staudacher, N. Raatz, S. Pezzagna, J. Meijer, F. Rein-

- hard, C. A. Meriles, and J. Wrachtrup, *Nat. Commun.* **6**, 8527 (2015).
- [23] X. Kong, A. Stark, J. Du, L. P. McGuinness, and F. Jelezko, *Phys. Rev. Applied* **4**, 024004 (2015).
- [24] F. Shi, Q. Zhang, P. Wang, H. Sun, J. Wang, X. Rong, M. Chen, C. Ju, F. Reinhard, H. Chen, et al., *Science* **347**, 1135 (2015).
- [25] F. Shi, F. Kong, P. Zhao, X. Zhang, M. Chen, S. Chen, Q. Zhang, M. Wang, X. Ye, Z. Wang, et al., *Nat. Methods* **15**, 697 (2018).
- [26] M. Flór, D. M. Wilkins, M. de la Puente, D. Laage, G. Cassone, A. Hassanali, and S. Roke, *Science* **386**, eads4369 (2024).
- [27] A. Lozovoi, H. Jayakumar, D. Daw, G. Vizkelethy, E. Bielejec, M. W. Doherty, J. Flick, and C. A. Meriles, *Nat Electron* **4**, 717 (2021).
- [28] K. Xu, D. Pagliero, G. I. López-Morales, J. Flick, A. Wolcott, and C. A. Meriles, *ACS Appl. Mater. Interfaces* **16**, 37226 (2024).